

# Naval Research Laboratory

Washington, DC 20375-5320



NRL/MR/6790-95-7647

## Observation of X-Ray Generation in a Proof-of-Principle Laser Synchrotron Source Experiment

A. TING  
R. FISCHER  
A. FISHER  
J. KRALL  
E ESAREY  
P. SPRANGLE

*Beam Physics Branch  
Plasma Physics Division*

K. EVANS

*George Mason University  
Fairfax, VA*

R. BURRIS

*R.S.I., Inc.  
Alexandria, VA*



DTIC QUALITY DETERMINED 2

February 15, 1995

Approved for public release; distribution unlimited.

19950301 128

# REPORT DOCUMENTATION PAGE

Form Approved  
OMB No. 0704-0188

Public reporting burden for this collection of information is estimated to average 1 hour per response, including the time for reviewing instructions, searching existing data sources, gathering and maintaining the data needed, and completing and reviewing the collection of information. Send comments regarding this burden estimate or any other aspect of this collection of information, including suggestions for reducing this burden, to Washington Headquarters Services, Directorate for Information Operations and Reports, 1215 Jefferson Davis Highway, Suite 1204, Arlington, VA 22202-4302, and to the Office of Management and Budget, Paperwork Reduction Project (0704-0188), Washington, DC 20503.

1. AGENCY USE ONLY (Leave Blank)	2. REPORT DATE	3. REPORT TYPE AND DATES COVERED	
	February 15, 1995	Interim	
4. TITLE AND SUBTITLE  Observation of X-Ray Generation in a Proof-of-Principle Laser Synchrotron Source Experiment			5. FUNDING NUMBERS
6. AUTHOR(S)  A. Ting, R. Fischer, A. Fisher, K. Evans,* R. Burris,** J. Krall, E. Esarey, and P. Sprangle			
7. PERFORMING ORGANIZATION NAME(S) AND ADDRESS(ES)  Naval Research Laboratory Washington, DC 20375-5320			8. PERFORMING ORGANIZATION REPORT NUMBER  NRL/MR/6790--95-7647
9. SPONSORING/MONITORING AGENCY NAME(S) AND ADDRESS(ES)  Office of Naval Research 800 North Quincy Street Arlington, VA 22217-5660			10. SPONSORING/MONITORING AGENCY REPORT NUMBER
11. SUPPLEMENTARY NOTES  *George Mason University, Fairfax, VA 22030-4444 **R.S.I., Inc., Alexandria, VA 22314			
12a. DISTRIBUTION/AVAILABILITY STATEMENT  Approved for public release; distribution unlimited.		12b. DISTRIBUTION CODE	
13. ABSTRACT (Maximum 200 words)  A Laser Synchrotron Source <sup>1</sup> (LSS) was proposed to generate short-pulsed, tunable x-rays by Thomson scattering of laser photons from a relativistic electron beam. A proof-of-principle (p.o.p) experiment on this LSS configuration is performed. An intense laser pulse ( $\lambda_0 = 1.053 \mu\text{m}$ ) is Thomson backscattered from a focussed relativistic electron beam. Time integrated x-ray signals from a photo-cathode/electron multiplier, at an electron beam energy of 650 keV and an x-ray photon energy of 20 eV, indicate an increase in the x-ray signals above the baseline by an amount comparable to the theoretically predicted value. This is the first observation of x-rays in the ten's of eV range generated by the Thomson scattering of near infrared photons from a relativistic electron beam.			
14. SUBJECT TERMS  X-ray Laser Synchrotron Source Thomson backscattering			15. NUMBER OF PAGES  13
			16. PRICE CODE
17. SECURITY CLASSIFICATION OF REPORT  UNCLASSIFIED	18. SECURITY CLASSIFICATION OF THIS PAGE  UNCLASSIFIED	19. SECURITY CLASSIFICATION OF ABSTRACT  UNCLASSIFIED	20. LIMITATION OF ABSTRACT  UL

# Observation of X-ray Generation in a Proof-of-Principle Laser Synchrotron Source Experiment

Thomson scattering of photons from electrons is well known to produce frequency upshifted photons in a narrow forward cone when the electron velocities are relativistic.<sup>2</sup> It has been proposed and experimentally demonstrated as a diagnostic tool for electron beam energy spread,<sup>3</sup> where optical photons were produced using a CO<sub>2</sub> laser and a 700 keV electron beam. Multi-MeV gamma ray production by Compton scattering of laser photons from GeV electron beams<sup>4</sup> was also reported. Recently, it was proposed that this mechanism can be used as an effective way of producing tunable, short pulse, near-monochromatic x-rays by backscattering infrared<sup>5</sup> and optical<sup>1</sup> photons from relativistic electron beams. This Laser Synchrotron Source (LSS) configuration<sup>1</sup> can be a compact x-ray source for many medical and material science applications. This compactness is recognized when the LSS is compared to conventional synchrotrons. The laser beam and MeV electron beam in a LSS correspond to the undulator/wiggler and the GeV beam in a synchrotron. Experiments have been proposed to study and implement this configuration at many institutions.<sup>6,7,8</sup> We are studying the various experimental issues involved in the LSS by carrying out a proof-of-principle (p.o.p.) experiment using the Naval Research laboratory (NRL) table-top terawatt (T<sup>3</sup>) laser and the NRL Febetron accelerator. This letter describes the experiment and the first observation of x-rays in the ten's of eV range generated by scattering of near infrared photons from relativistic electrons in the LSS configuration.

A schematic diagram of the p.o.p. LSS experiment is shown in Figure 1. The electron beam is magnetically focussed into the interaction region. The NRL T<sup>3</sup> laser is focussed and directed onto the electron beam in the counter-streaming direction. The synchrotron radiation, which is frequency-upshifted by  $\sim 4\gamma^2$ , where  $\gamma$  is the relativistic factor of the electron beam, has a central wavelength of  $\sim 30\text{-}60$  nm ( $\sim 16\text{-}35$  eV) in this experiment, depending on the electron beam energy ( $\sim 0.6\text{-}1$  MeV). It is collected by a bundle of glass capillary tubes and detected by a modified electron multiplier tube (EMT) at the center of the vacuum chamber. A CCD camera is used to align the electron beam.

The electron beam is produced by a compact Febetron pulser which is rated to deliver a nominal 0.6 MV, 55ns pulse into a matched load of  $100\ \Omega$  impedance. We operated the Febetron with a mismatched diode to increase

the peak output voltage on the diode. Depending on the charging voltage on the Febetron, peak voltages of  $\sim$ 0.6-1 MV and  $\sim$ 2 kA of diode current can be obtained. A schematic diagram of the diode region is shown in Figure 2. The cathode is a metal cone with a sphere of  $\sim$ 4 mm diameter at the apex. This simulates a point source of electron emission. The 2 cm graphite anode aperture discards the outer portion of the beam so that only those electrons with small angular divergence and low perpendicular energy are selected. A pulsed thin solenoid is located at the anode to act as a magnetic lens for focussing the electron beam at the second aperture which is the laser/electron interaction region. The Febetron is fired at a field of  $\sim$ 700 G to focus electrons with energies  $\sim$ 650 keV. Four solenoids are placed around the beam tube to steer the electron beam in the transverse plane using fields of up to 500 G on-axis. A Rogowski coil measures the current transmitted past the output (interaction) aperture. It showed the transmitted current has a pulse length of  $\sim$ 20 nsec. The electron beam is then directed onto the walls of a graphite/lead beam dump using permanent magnets. A 2  $\mu$ m-thick piece of mylar is placed at the lead anode aperture to block x-ray photons from the cathode plasma. It introduces minimal effects on the focussability of the electron beam.

Three techniques are used to measure the electron beam size and current density at the second aperture. First, graphite apertures of varying sizes (2-9 mm) are placed at the interaction region and the transmitted current is measured. Secondly, radiachromic nylon film is placed in the path of the beam and darkened with 1 shot from the Febetron. Approximately 230  $\mu$ m of copper is used as a filter to block low energy electrons for improved contrast on the film. A third method uses a copper-filter-backed fluorescent sheet which is placed at the output aperture of the electron beam. The fluorescence is viewed with a CCD camera. At 650 kV on the Febetron, a central peak intensity area of 2 mm in diameter is observed. The corresponding beam current is 20 A. The electron beam parameters are summarized in Table 1.

The NRL T<sup>3</sup> laser is based on the chirped pulse amplification technique.<sup>9</sup> It produces 1-2 J of laser energy at 1.053  $\mu$ m with a pulse length of  $\sim$ 0.5 nsec before compression or  $\sim$ 0.8 psec after compression. The laser parameters are listed in Table 1. The beam is focussed using a 75 cm plano-convex lens to a spot size of 60  $\mu$ m (1.5 times diffraction limited). The focal

spot is arranged to be ~1.5 cm in front of the interaction region so that the laser beam diverges to a spot size of ~1 mm at the interaction region. The laser beam intersects the electron beam at an angle of approximately 8 degrees so that the laser will miss the Febetron cathode and the optics do not block the EMT. As shown in Figure 2, a piece of OD2 filter glass is placed on the front portion of the anode as a laser beam dump to absorb the spent laser beam. Data were taken with the laser delivering the uncompressed pulse to the interaction chamber. The uncompressed pulse has a lower peak intensity and therefore reduces the risk of laser breakdown at the laser beam dump which would appear as a spurious signal on the EMT.

The x-ray detector is a modified, commercially available EMT (ETP model#AF150H) which has 21 dynode stages. Some of its specifications and operating parameters are listed in Table 1. We calibrated the gain of the EMT with a weak radioactive source to be  $\sim 1 \times 10^6$  at our bias voltage of 1900 V. The response time of the EMT is 5 nsec, so that all measurements of LSS radiation are time-integrated regardless of the pulse length of the laser. The internal delay of the EMT is 40 nsec, so care must be taken when analyzing the relative timing of signals on the oscilloscope. Aluminum oxide dynodes are used in the EMT which, unlike other dynode materials, do not degrade when exposed to air for extended periods of time. For pulsed operation, capacitors are added to the last three stages of the tube to avoid saturation. As shown in Figure 1, the EMT is oriented perpendicular to the incident x-rays, where a concave photocathode has been installed. This photocathode is coated with carbon and biased at -2500 V. Carbon photocathode is particularly sensitive to the desired x-ray radiation at 20 eV (efficiency ~5 %). Higher energy x-rays which are generated when the electron beam intersects the apertures or the beam dump are not efficiently collected by this photocathode. Glass capillary tubes are used for collimating the x-rays. These glass capillary tubes have an inner diameter of ~1 mm. The acceptance of these capillary tubes is highly directional and therefore discriminates against the background x-rays generated in the electron beam dump. They allow the passage of soft x-rays in the range of 10-100 eV. The sensitivity of the modified EMT was tested with soft x-rays from a laser-produced plasma by focussing 1 mJ of laser energy onto a graphite target placed at the interaction aperture. The collection efficiency of the glass capillary tubes was measured to be ~25 %.

Availability Codes	
Dist	Avail and/or Special
A-1	

The LSS x-ray signal in this experiment can be estimated as follows. The peak power of the x-rays from an LSS is given by<sup>1</sup>

$$P_x[W] = 1.05 \times 10^{-6} L[\text{cm}] J[\text{A/cm}^2] (2E_b[\text{MeV}] + 1)^2 P_0[\text{GW}],$$

where  $L$  is the interaction length of a single electron,  $J$  is the current density,  $E_b$  is the electron beam energy, and  $P_0$  is the laser power. Here we have assumed that the laser spot is smaller than the electron beam spot. Consider the experimental parameters of  $J=600 \text{ A/cm}^2$ ,  $E_b=0.65 \text{ MeV}$ ,  $P_0=2 \text{ GW}$ , and a laser pulsewidth  $\tau_0$  of 0.5 nsec. The interaction length  $L$  of a single electron is given by the depth of focus of the electron beam which is  $\sim 1 \text{ cm}$ , yielding a peak x-ray power of  $\sim 6.6 \times 10^{-3} \text{ W}$ . The x-ray pulse length,  $\tau_x$ , is equal to the laser pulse length of 0.5 nsec, and therefore the total energy of the LSS x-ray pulse depends only on the laser energy and not on its pulse length. Assuming a photon energy of 20 eV, it is estimated that  $\sim 1 \times 10^6$  photons are generated. For individual electrons, the synchrotron radiation is emitted in a cone of half angle  $1/\gamma \sim 25^\circ$ . However, the electron beam has a convergence half angle of  $\sim 15^\circ$  at the focus, leading to an  $\sim 40^\circ$  half angle for the exiting LSS photons. If the detector is placed 35 cm away from the interaction region with an acceptance of  $1 \text{ cm}^2$ , then  $\sim 5.5 \times 10^{-4}$  of the photons enter the detector. Thus, approximately 550 LSS photons should strike the capillary tube collimator. Considering the efficiencies of the capillary tubes and the photocathode, and the gain of the EMT, a 10 nsec EMT pulse with a  $50 \Omega$  termination should produce a 5.5 mV difference in x-ray signal when the Febetron is fired with and without the laser.

Data were taken from oscilloscope traces of the EMT output at the predicted instance of LSS x-ray occurrence. The laser timing is set by observing the x-ray signals created by the laser breakdown of a graphite target at the interaction point. The laser has negligible jitter in timing. The timing for the Febetron is achieved by recording the x-ray produced by the electron beam on a thin target at the interaction point. The Febetron has a jitter of  $\sim 2 \text{ nsec}$ . The data, shown in Figure 3, is a collection of uncorrelated shots, showing the total x-ray signal from the EMT. The triangular dots are the x-ray signals observed when only the Febetron is firing, referred to as F data. The open

squares are x-ray signals with both the laser and febetron firing, referred to as L+F data. The L+F data has a mean of 36.2 mV with a standard deviation (s.d.) of 2.8 mV, while the F data has a mean of 32.7 mV and a s.d. of 1.3 mV. The L+F data, as expected, is greater than the F data. The difference of the two means is 3.5 mV, which is ~65% of the expected 5.5 mV difference in the two signals. When the x-ray signals are examined at 10 nsec delay (twice the EMT response time) from the synchronized laser-electron interaction time, there is no observed difference in the x-ray signals. Numerous other null tests were performed. No x-ray signals are detected when only the laser is fired. No increase of the Febetron x-ray signal is detected when the laser is fired simultaneously but blocked from interacting with the electron beam. No EMT signals are detected when the capillary tubes are blocked.

There are two major difficulties in this p.o.p. LSS experiment. The first one is that the x-ray photons in this experiment are in a particularly difficult region of the electromagnetic spectrum for detection. The choice of the photocathode material is critical. One needs to select a material for which the photon energy of maximum photoelectron production coincides with the energy of the photons to be measured, and which has a relatively narrow sensitivity peak. For example, carbon works well at 20 eV because its sensitivity peaks at 16 eV and then rapidly falls off to become negligible above 30 eV. This consideration dictates the operating voltage of the Febetron. We have tried to detect 35 eV LSS x-rays using 1 MeV electron beams from the Febetron and a Cesium Iodide (CsI) photocathode. CsI's sensitivity has a relatively high peak at 20 eV and the peak is broad enough that it is still sensitive at photon energies around 35 eV. However, its sensitivity curve also has a very broad and substantial hump extending from ~40 eV to over 100 eV. This allows it to collect enough background x-rays to obscure the LSS x-ray signal that we are trying to detect. A low dispersion grating would be desirable to select incoming x-ray photons within the favorable energy range. However, the photon flux at the detector would be sacrificed. The second difficulty involves the reduction of the background x-ray signal which is proportional to the dumped electron beam current. However, reducing the electron current also reduces the desired x-ray signal. Hence, careful design and construction of the electron beam dump was necessary to improve the signal to noise ratio. Another difficulty in the experiment is the stability of

the electron beam focus. The electron beam originates from an explosive cathode plasma created at the surface of the field emission cathode. The magnetic focussing system maps spurious emission spots on the cathode to the beam focus at the interaction region. Another major source of instability of the beam focus is that pulsed power devices like the Febetron do not have very reproducible voltage profiles. Since the magnetic lens is very dispersive in electron energies, an unstable beam energy profile will lead to instabilities in the beam focus. A more reliable electron beam accelerator is therefore very desirable. Accelerators such as radio-frequency (RF) linacs using thermionic cathodes or high-brightness photocathodes will alleviate some of the difficulties we have accounted. The higher current densities at focus from these brighter electron guns would also generate higher x-ray photon fluxes.

In conclusion, we have performed a p.o.p experiment on the LSS using the NRL T<sup>3</sup> laser and the NRL Febetron accelerator. X-rays in the 20 eV energy range were observed to be generated by Thomson backscattering of 1.053  $\mu$ m photons from 650 keV relativistic electrons. The results show that when the laser and electron beams are synchronized and aligned, x-ray signals are observed to be higher than the baseline where only the electron beam is fired. The increase in the x-ray signal is consistent with the predicted value calculated from the operating parameters of the laser and electron beam. Further experiments are under design to produce x-rays in the 100's of eV range using more energetic electron beams from RF gun structures.

The authors would like to acknowledge helpful discussions with R. Elton, B. Hafizi, C. Roberson, C. Manka, B. Ripin and J. Grun. The authors are also grateful for technical assistance from A. Kinkead, L. Daniels and E. Goodman. This work is supported by the Office of Naval Research.

## References

1. P. Sprangle, A. Ting, E. Esarey and A. Fisher, *J. Appl. Phys.* **72**, 5032 (1992).
2. J.D. Jackson, "Clasical Electrodynamics," (Wiley, NY, 1975).
3. S.C. Chen and T. Marshall, *Phys. Rev. Lett.* **52**, 425 (1984); S.C. Chen and T.C. Marshall, *IEEE J. Quan. El.* **QE-21**, 924 (1985).
4. O.F. Kulikov, Y.Y. Telnov, E.I. Filippov and M.N. Yakimenko, *Phys. Lett.* **13**, 344 (1964); C. Bemporad, R.H. Milburn, N. Tanaka and M. Fotino, *Phys. Rev.* **138**, B1546 (1965); C.K. Sinclair, J.J. Murray, P.R. Klein and M. Rabin, *IEEE Trans. Nucl. Sci.* **NS-16**, 1065 (1969).
5. F.E. Carroll, J.M. Waters, R.R. Price, C.A. Brau, C.F. Roos, N.H. Tolk, D.R. Pickens and W.H. Stephens, *Investigative Radiology* **25**, 465 (1990).
6. P. A. Tompkins, C. A. Brau, W.W. Dong and J.W. Waters, *Proc. 1993 Part. Acc. Conf.*, 1448 (1993).
7. W. Leeman, 6th Workshop on Adv. Acc. Concepts, Lake Geneva, Wisc., June 12-18, 1994.
8. A.C. Melissinos, private communication.
9. P. Maine, D. Strickland, P. Bado, M. Pessot and G. Mourou, *IEEE J. Quan. Electron.* **QE-24**, 398 (1988).

**Febetron electron beam parameters:**

Beam voltage	650	kV
Cathode current	2	kA
Cathode diameter	4	mm
Anode-cathode gap	3	cm
Magnetic field	0.7	kG
Focussed current	20	A
Focussed spot dia.	2	mm
Current density	0.6	kA/cm <sup>2</sup>

**T<sup>3</sup> laser parameters:**

Wavelength	1.053	μm
Energy	1	Joule
Pulse width (compressed)	0.8	psec
Pulse width (uncompressed)	0.5	nsec
Beam size	4.5	cm
Beam quality	1.5	$\theta_{\text{diff}}$

**Electron Multiplier Parameters:**

Current Gain	1×10 <sup>6</sup>
Number of Stages	21
Bias	1.9 kV
Aperture	12×7 mm <sup>2</sup>
Dynode Coating	Al <sub>2</sub> O <sub>3</sub>
Risetime	5 nsec
Delay	40 nsec

Table 1: Parameters of the p.o.p. LSS experiment.

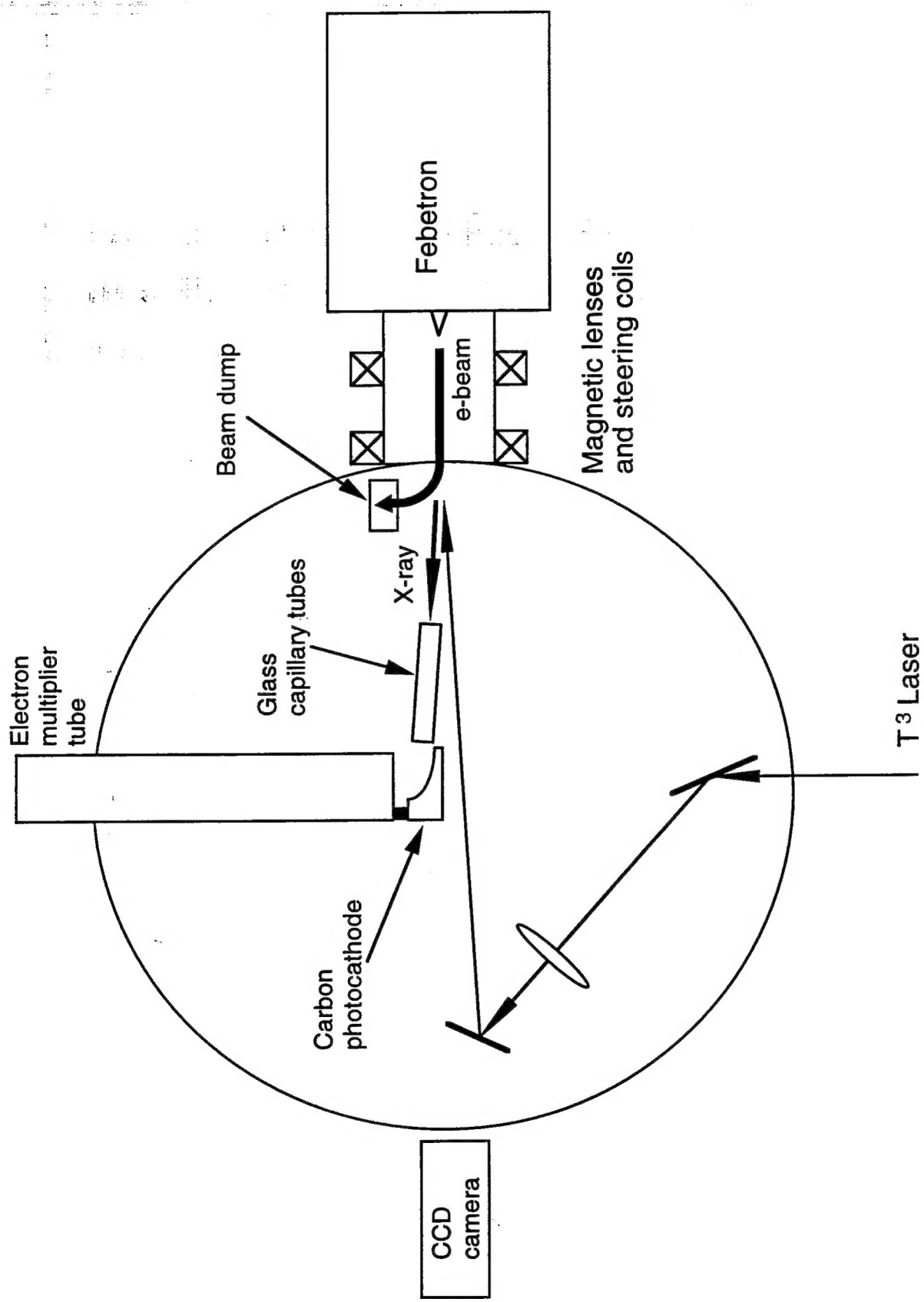


Figure 1: Schematic diagram of the LSS p.o.p. experiment

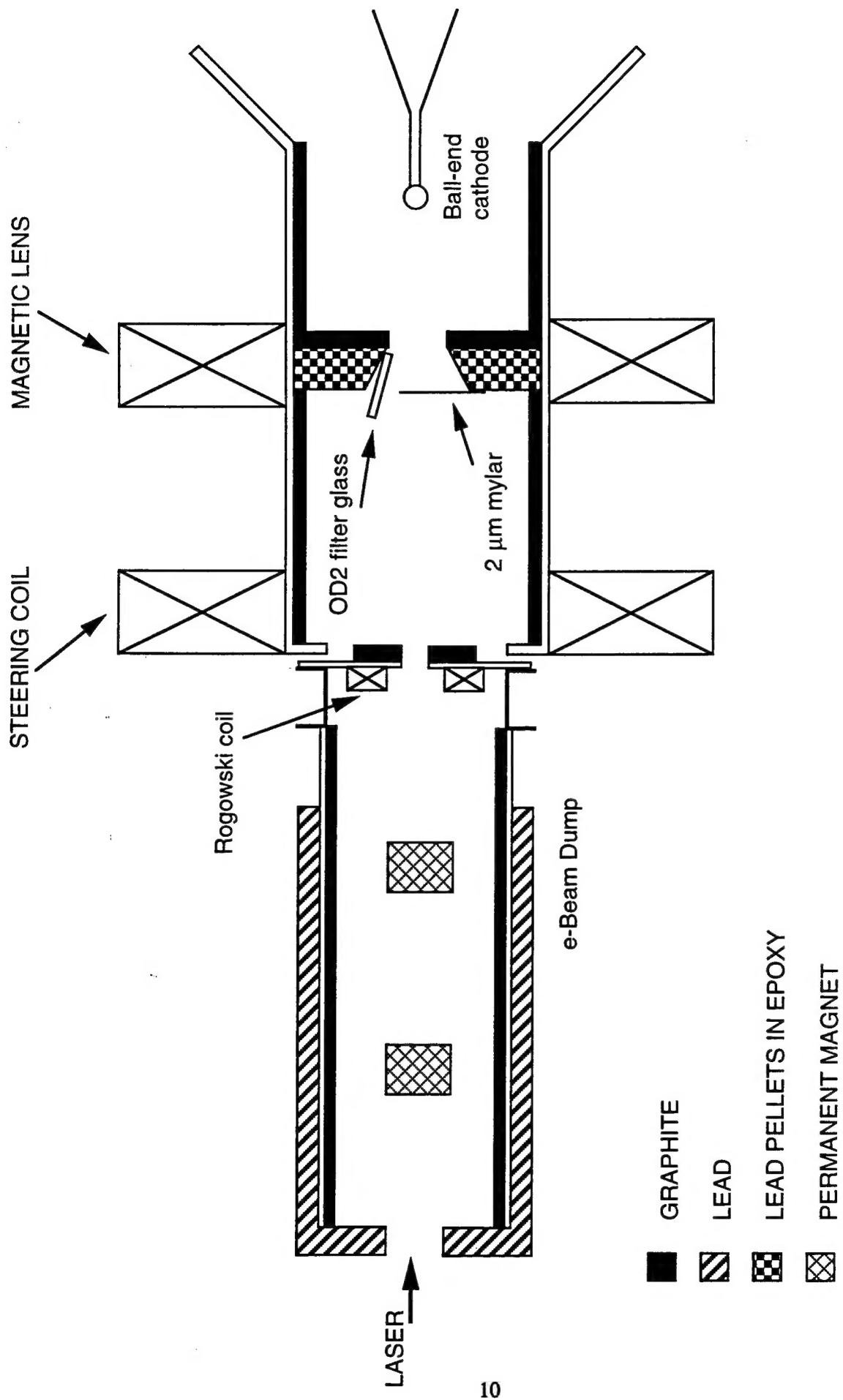


Figure 2: Schematic diagram of the diode region of the Febeletron

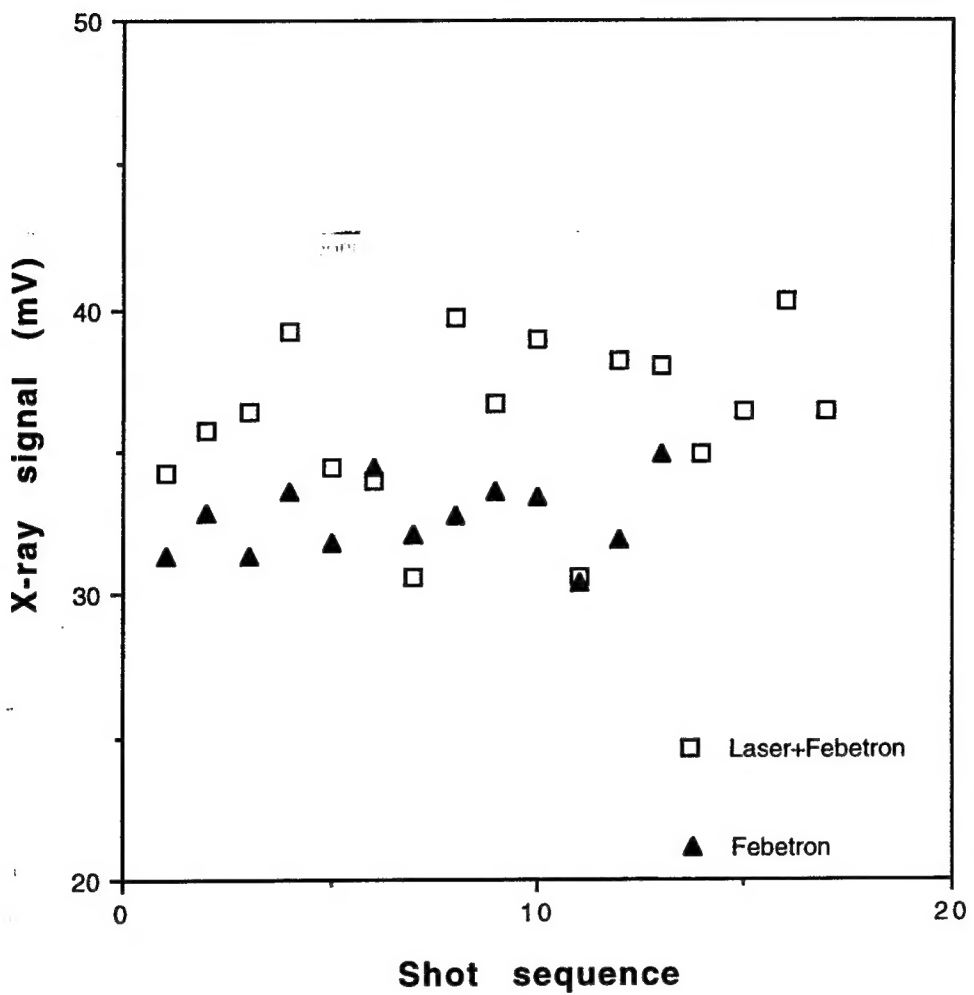


Figure 3: X-ray signals from p.o.p. LSS experiment